Molecular Biology of the Cell
Vol. 19, 5047–5058, December 2008

Cardiolipin Mediates Cross-Talk between Mitochondria and the Vacuole

Shuliang Chen,* Maureen Tarsio,† Patricia M. Kane,† and Miriam L. Greenberg*

*Department of Biological Sciences, Wayne State University, Detroit, MI 48202; and †Department of Biochemistry and Molecular Biology, SUNY Upstate Medical University, Syracuse, NY 13201

Submitted May 15, 2008; Revised August 22, 2008; Accepted September 8, 2008
Monitoring Editor: Thomas D. Fox

Cardiolipin (CL) is an anionic phospholipid with a dimeric structure predominantly localized in the mitochondrial inner membrane, where it is closely associated with mitochondrial function, biogenesis, and genome stability (Daum, 1985; Janitor and Subik, 1993; Jiang *et al*., 2000; Schlame *et al*., 2000; Zhong *et al*., 2004). Previous studies have shown that yeast mutant cells lacking CL due to a disruption in *CRD1*, the structural gene encoding CL synthase, exhibit defective colony formation at elevated temperature even on glucose medium (Jiang *et al*., 1999; Zhong *et al*., 2004), suggesting a role for CL in cellular processes apart from mitochondrial bioenergetics. In the current study, we present evidence that the *crd1*Δ mutant exhibits severe vacuolar defects, including swollen vacuole morphology and loss of vacuolar acidification, at 37°C. Moreover, vacuoles from *crd1*Δ show decreased vacuolar H^+-ATPase activity and proton pumping, which may contribute to loss of vacuolar acidification. Deletion mutants in *RTG2* and *NHX1*, which mediate vacuolar pH and ion homeostasis, rescue the defective colony formation phenotype of *crd1*Δ, strongly suggesting that the temperature sensitivity of *crd1*Δ is a consequence of the vacuolar defects. Our results demonstrate the existence of a novel mitochondria-vacuole signaling pathway mediated by CL synthesis.

INTRODUCTION

In eukaryotes, the anionic phospholipid cardiolipin (CL) and its precursor phosphatidylglycerol (PG) are synthesized and localized exclusively in the mitochondrial inner membrane (Hoch, 1992; Schlame *et al*., 2000). In the yeast *Saccharomyces cerevisiae*, the biosynthesis of CL requires three sequential reactions performed by phosphatidylglycerol phosphate synthase (encoded by *PGS1*), phosphatidylglycerol phosphate phosphatase, and CL synthase (encoded by *CRD1*) (Gu *et al*., 2002). The fatty acyl species of CL are remodeled by taffazin (*TAZ1*) (Li *et al*., 2007). The specific association of CL with individual mitochondrial proteins and complexes is important for their optimal function and structural integrity. Dissociation of CL from these proteins results in inactivation of the complexes and/or decrease of the protein activities, underscoring the important role of CL in mitochondrial function (Yu and Yu, 1980; Drees and Beyer, 1988; Robinson *et al*., 1990; Hayer-Hartl *et al*., 1992; Beyer and Nuscher, 1996; Gomez and Robinson, 1999; Sedlak and Robinson, 1999).

The last several years have witnessed an increase in studies using yeast mutants altered in CL synthesis and remodeling to elucidate the functions of the CL pathway. The importance of CL remodeling is becoming clearer from studies with the *taz1*Δ mutant, which exhibits biochemical defects similar to those observed in the severe genetic disorder Barth syndrome, in which tafazzin is mutated. Loss of tafazzin in yeast and human cells leads to defects in CL metabolism, including aberrant CL fatty acyl composition, accumulation of monolysocardiolipin, and reduced total CL levels (Vreken *et al*., 2000; Schlame *et al*., 2002; Valianpour *et al*., 2005). The yeast *taz1*Δ mutant also exhibits ethanol sensitivity at elevated temperature, perturbation of coupling and respiratory control, and increased protein carbonylation during respiratory growth conditions (Gu *et al*., 2004; Ma *et al*., 2004; Chen *et al*., 2008). The *crd1*Δ mutant, which lacks CL, has more severe defects in growth and mitochondrial function than does the *taz1*Δ mutant. Mitochondria from the *crd1*Δ mutant exhibit reduced membrane potential, perturbed coupling, instability of electron transport chain supercomplexes and impaired protein import (Jiang *et al*., 2000; Koshkin and Greenberg, 2000, 2002; Zhang *et al*., 2002, 2005; Pfeiffer *et al*., 2003). In addition, the *crd1*Δ mutant in some genetic backgrounds shows a loss of viability at elevated temperature and cannot form colonies from single cells even during growth on glucose, suggesting that CL plays an essential role in cellular function apart from mitochondrial bioenergetics (Jiang *et al*., 1999; Zhong *et al*., 2004). The growth and viability defects of *crd1*Δ are not apparent at optimal temperatures, most likely because PG, which accumulates markedly in the mutant, can substitute for some functions of CL (Chang *et al*., 1998b; Zhong *et al*., 2004). The *pgs1*Δ mutant, which lacks both PG and CL, has a more severe growth defect compared with *crd1*Δ or *taz1*Δ. Disruption of *PGS1* results in the spontaneous loss of mitochondrial DNA (mtDNA), cell inviability at 37°C, and defective cell wall synthesis (Chang *et al*., 1998a; Dzugasova *et al*., 1998; Zhong *et al*., 2005, 2007). These findings indicate that anionic phospholipids play an important role not only in mitochondrial bioenergetics but also in numerous cellular processes that are not generally associated with mitochondrial function.

This article was published online ahead of print in *MBC in Press* (http://www.molbiolcell.org/cgi/doi/10.1091/mbc.E08–05–0486) on September 17, 2008.

Address correspondence to: Miriam L. Greenberg (mlgreen@sun.science.wayne.edu).

Abbreviations used: ACMA, 9-amino-6-chloro-2-methoxyacridine; CL, cardiolipin; PG, phosphatidylglycerol; WT, wild type.

Genetic studies to identify suppressors of the *pgs1*Δ growth defects led to the unexpected finding that loss of mitochondrial anionic phospholipids PG and CL results in perturbation of cell wall biosynthesis (Zhong *et al.*, 2005). Consistent with this finding, disruption of *PGS1* leads to a defective protein kinase C (PKC) signaling pathway, decreased glucan synthesis, and an aberrant cell wall (Zhong *et al.*, 2007). Osmotic stabilization of the cell wall by supplementation with 1 M sorbitol can rescue these phenotypes. Interestingly, defective colony formation in *crd1*Δ is also rescued by 1 M sorbitol (Zhong *et al.*, 2005), suggesting that temperature sensitivity of *crd1*Δ may be due at least in part to a cell wall defect. However, the *crd1*Δ mutant does not exhibit increased sensitivity to cell wall-perturbing agents and contains only slightly reduced levels of glucan, indicating that the *crd1*Δ mutant maintains cell wall integrity and that the accumulation of PG in *crd1*Δ cells satisfies the anionic phospholipid requirement for cell wall biogenesis (Zhong *et al.*, 2007). Therefore, the molecular mechanisms underlying suppression of temperature sensitivity in *crd1*Δ by hyperosmotic stress (1 M sorbitol) are not known.

Studies of global responses to hyperosmotic stress reveal that to adapt to high extracellular osmolarity, yeast cells adjust expression of numerous genes and protein synthesis to maintain or reestablish cellular functions (Varela *et al.*, 1992; Blomberg, 1995; Norbeck and Blomberg, 1996; Posas *et al.*, 2000; Rep *et al.*, 2000; Yale and Bohnert, 2001). Most likely, osmoadaptation mechanisms compensate *crd1*Δ for defects at elevated temperature and contribute to survival of the mutant. The initial effect of hyperosmotic stress on living cells is a rapid efflux of water (Hohmann, 2002). The yeast vacuole plays a key role in avoiding the fatal consequences of high external osmolarity and decrease in turgor pressure. To achieve long-term adaptation to environmental variation, rapid adjustments in vacuolar volume resulting from uptake or release of water and solutes are critical in balancing cytoplasmic ion concentrations (Klionsky *et al.*, 1990; Latterich and Watson, 1993). Loss of regulation of ion transport across the membrane of the vacuole may create an osmotic imbalance, causing water from the cytosol to diffuse in and swell the vacuole (Efe *et al.*, 2005). Because 1 M sorbitol contributes high external osmolarity that can affect ion homeostasis, the finding that 1 M sorbitol suppresses defective colony formation in *crd1*Δ provided a clue that the colony formation defect in the mutant may be due to perturbation of the vacuole.

Consistent with this hypothesis, we found that *crd1*Δ exhibited severe vacuolar defects at elevated temperature, including loss of vacuolar acidification and enlarged vacuolar morphology accompanied by swollen cell size. The rescue of temperature sensitivity and vacuolar defects by 1 M sorbitol indicated that high external osmolarity restored cell viability of *crd1*Δ by restoration of vacuolar functions. Further studies demonstrated that vacuoles from *crd1*Δ showed low vacuolar type H^+-ATPase (V-ATPase) activity and reduced proton transport. Interestingly, disruption of *RTG2* rescued vacuolar defects by increasing V-ATPase activity and coupling, and suppressed the single colony formation defect in *crd1*Δ at elevated temperature. Suppression was also achieved by deletion of *NHX1*, a gene encoding the late endosomal/prevacuolar Na^+/H^+ exchanger generally involved in export of protons in exchange for cytosolic Na^+ or K^+ (Ali *et al.*, 2004). The *crd1*Δ*nhx1*Δ double mutant restored vacuolar acidification, morphology and single colony formation defects at high temperature, a further indication that the *crd1*Δ mutant is subject to impaired cytosolic and vacuolar ion homeostasis. These studies identify for the first time the existence of a novel mitochondria–vacuole signaling pathway mediated by the synthesis of CL.

MATERIALS AND METHODS

Yeast Strains, Growth Media, and Growth Condition

The *S. cerevisiae* strains used in this work are listed in Table 1. Synthetic complete medium (SD) contained adenine (20.25 mg/l), arginine (20 mg/l), histidine (20 mg/l), leucine (60 mg/l), lysine (200 mg/l), methionine (20 mg/l), threonine (300 mg/l), tryptophan (20 mg/l), and uracil (20 mg/l), yeast nitrogen base without amino acids (Difco, Detroit, MI), and glucose (2%). Synthetic drop out medium contained all of the above-mentioned ingredients except the amino acid as a selectable marker. Complex media (YPD) contained yeast extract (1%), peptone (2%), and glucose (2%). YPDS medium was YPD supplemented with 1 M sorbitol. Solid medium contained agar (2%) in addition to the above-mentioned ingredients.

The deletion mutants were constructed as follows. The entire open reading frame of the target gene was replaced by *KanMX4* by using polymerase chain reaction (PCR)-mediated homologous recombination in the wild-type strain. The *KanMX4* cassette was amplified from pUG6 by using primers consisting of 50 nucleotides identical to the target gene flanking regions at the 5′ end and 21 nucleotides for the amplification of the *KanMX4* gene at the 3′ end. The PCR product was transformed into the wild-type strain, and transformants were selected on YPD media containing G418 (200 μg/ml). Disruption of the target gene was confirmed by PCR using primers against the target gene coding sequences.

Plasmid Construction

To construct an *RTG2*-overexpressing plasmid, a 1775-base pairs sequence containing the entire open reading frame of *RTG2* was amplified from yeast genomic DNA by using SacI-tagged primer 18RTG2-f (5′-AAAGTG-GAGCTCTGCCACAAATGTCAACACTTA-3′) and BamHI-tagged primer 18RTG2-r (5′-GACTAGGGATCCTTATTCTTCATAAAATTGCACGC-3′). The

Table 1. Yeast strains and plasmids used in this study

Strain/plasmid	Characteristics or genotype	Source or reference
FGY3	*MAT* α, *ura 3-52, lys2-801, ade2-101, trp1*Δ*1, his3*Δ*200, leu2*Δ*1*	Jiang *et al.* (1997)
FGY3 ρ°	*rho*° mutant derived from FGY3	Zhong *et al.* (2005)
FGY2	*MAT* α, *ura 3-52, lys2-801, ade2-101, trp1*Δ*1, his3*Δ*200, leu2*Δ*1, crd1*Δ*::URA3*	Jiang *et al.* (1997)
FGY3 *rtg2*Δ	Derivative of FGY3, *rtg2*Δ*::KanMX4*	This study
FGY2 *rtg2*Δ	Derivative of FGY2, *rtg2*Δ*::KanMX4*	This study
FGY3 *rtg3*Δ	Derivative of FGY3, *rtg3*Δ*::KanMX4*	This study
FGY2 *rtg3*Δ	Derivative of FGY2, *rtg3*Δ*::KanMX4*	This study
FGY3 *nhx1*Δ	Derivative of FGY3, *nhx1*Δ*::KanMX4*	This study
FGY2 *nhx1*Δ	Derivative of FGY2, *nhx1*Δ*::KanMX4*	This study
FGY3 *cnb1*Δ	Derivative of FGY3, *cnb1*Δ*::KanMX4*	This study
FGY2 *cnb1*Δ	Derivative of FGY2, *cnb1*Δ*::KanMX4*	This study
pYPGK18	2 μm, *LEU2*	Vaz *et al.* (2003)
pYPGK18-RTG2	Derivative of pYPGK18, expresses *RTG2* from PGK1 promoter	This study

Table 2. Real-time PCR primers used in this study

Gene	Primers	Sequence	Product length (bp)
ACT1	Forward	TCGTGCTGTCTTCCCATCTATCG	218
	Reverse	CGAATTGAGAGTTGCCCCAGAAG	
RTG2	Forward	TAGCCGGCTGTCATGGATTATCTC	287
	Reverse	TAAACTGGTCTCCACCTCACTACG	
CIT2	Forward	CGGAACTACCTAGTCATGTCGTTCA	309
	Reverse	CATCCTTAGAACCAATCAAGTTGACCAG	
DLD3	Forward	ACGTCAGGGTCCAATAAGAGACAC	258
	Reverse	CAAACCGGCTGCGTTTAATCTCTC	
CMD1	Forward	CGCCCAGTGAAGCAGAAGTAAATG	280
	Reverse	ATCTCGCCTGATCCATCACTAACC	
CNA1	Forward	AGTAACAGGCTTCCCGAGCTTAATA	274
	Reverse	CGCAGCTTTGGGTTCCGAT	
CNA2	Forward	GACTTTGGGCTTTCCCTCTCTTTTG	282
	Reverse	CCAACTAATTCTTCAATGACGGGGG	
CNB1	Forward	CCCTCTTGCTGGACGTATAATGGA	349
	Reverse	CAATGTCAGACTCTTGGCCACTTC	

PCR products were ligated to pYPGK18 (2 μm, *LEU2*) cut with SacI and BamHI, downstream of the *PGK1* promoter.

Fluorescence and Microscopic Analysis

All microscopy was performed using an Olympus BX41 epifluorescence microscope. Images were acquired using an Olympus Q-Color3 digital charge-coupled device camera operated by QCapture2 software. Pictures in the same pattern were taken at the same magnification (1,000×).

To visualize vacuolar morphology in vivo, yeast cells were labeled with *N*-[3-triethylammoniumpropyl]-4-[*p*-diethylaminophenylhexatrienyl] pyridinium dibromide (FM4-64) (Invitrogen, Carlsbad, CA) as described previously, with a few modifications (Vida and Emr, 1995). Mid-log phase cells were harvested and resuspended in fresh media to an optical density A_{550} of 1.0. FM4-64 was then added to a final concentration of 16 μM. After incubation with FM4-64 at room temperature for 15–30 min, cells were washed twice with fresh media and viewed with fluorescence microscopy.

To assess vacuole acidification in vivo, yeast cells were stained with quinacrine as described by Weisman *et al*. (1987), with minor modifications. Yeast cells grown to the mid-log phase were harvested by centrifugation at 2000 × *g*. Quinacrine was added to a final concentration of 200 μM to cells resuspended in YPD buffered at pH 7.6. Cells were incubated at room temperature for 5 min and washed with 50 mM phosphate-buffered saline containing 2% glucose, pH 7.6. Cells were examined immediately under the fluorescence microscope using an Olympus BX41 NIB filter.

Isolation and Analysis of Vacuolar Vesicles

Wild-type and mutant cells were grown overnight in YPD at 30°C to early log phase. For biochemical comparison of wild-type and crd1Δ mutant vacuoles at 30°C, vacuolar vesicles were then isolated from the cells as described previously (Roberts *et al*., 1991). To determine the effects of a shift to 37°C, the overnight cultures were diluted into prewarmed YPD medium and growth at 37°C was continued for 3.5 h. (At this time, enlarged vacuoles had begun to occur in the *crd1*Δ mutant strain, and the diluted cultures were at a growth phase comparable with that used for isolation of vacuolar vesicles from cells maintained at 30°C.) Cells were then converted to spheroplasts and vacuolar vesicles were isolated by Ficoll gradient centrifugation as described previously (Roberts *et al*., 1991), except that recovery of the spheroplasts before lysis was carried out by incubating the cells in YPD containing 1.2 M sorbitol at 37°C for 20 min rather than 30°C. Vacuolar vesicles were assayed for ATPase activity, and the activity sensitive to 200 nM concanamycin A was taken as V-ATPase activity. Proton pumping was assayed by the 9-amino-6-chloro-2-methoxyacridine (ACMA) fluorescence quenching assay as described previously (Liu *et al*., 2005); pumping was initiated by addition of ATP and Mg^{2+} to final concentrations of 0.5 and 1 mM, respectively, and reversed after addition of 200 nM concanamycin A. Total vacuolar protein was measured by Lowry assay.

Levels of V-ATPase V_1 subunits A and B, V-ATPase V_0 subunit a, and alkaline phosphatase (ALP) in isolated vacuolar vesicles were compared by immunoblot as described previously (Kane *et al*., 1992). Vesicles were solubilized and equivalent amounts of total vacuolar vesicle protein from each strain and condition (5 μg for detection of the V-ATPase A and B subunits and 10 μg for detection of the V-ATPase a subunit and ALP) were separated by SDS-polyacrylamide gel electrophoresis, and transferred to nitrocellulose. V_1 subunits A and B were detected by mouse monoclonal antibodies 8B1 and 13D11, and V_0 subunit a was recognized by monoclonal antibody (mAb) 10D7 (Kane *et al*., 1992). ALP was detected by mAb 1D3 (Invitrogen). All of the primary antibodies were visualized using alkaline phosphatase-conjugated goat anti-mouse secondary antibody (Promega. Madison, WI) followed by colorimetric development.

Real-Time PCR

Yeast cultures (10 ml) were grown to the early stationary phase, cells were harvested, and total RNA was isolated using the RNeasy Mini kit (QIAGEN, Valencia, CA). The RNA samples were treated with DNase from a DNA-free kit (Ambion, Austin, TX) to remove contaminating genomic DNA. cDNAs were synthesized with a Reverse-iT 1st Strand Synthesis kit (ABgene, Epsom, Surrey, United Kingdom) according to the manufacturer's protocol. Real-time PCR reactions were performed in a 50-μl volume using ABsolute quantitative PCR SYBR Green Mix (ABgene) in a 96-well plate. Duplicates for each sample were included for each reaction. The real-time PCR primers used are listed in Table 2 and Supplemental Table S1. *ACT1* was used as the internal control and the RNA level of the gene of interest was normalized to *ACT1* levels. PCR reactions were initiated at 95°C for 10 min for denaturation followed by 40 cycles consisting of 30 s at 95°C and 60 s at 57°C.

RESULTS

Disruption of CRD1 Leads to Vacuolar Defects at Elevated Temperature

Previous studies have shown that the *pgs1*Δ mutant forms enlarged cells with more spherical appearance and larger cell size than wild type (WT), due to cell wall defects (Zhong *et al*., 2005). Supplementation with 1 M sorbitol stabilizes the cell wall and rescues growth and morphological defects in the mutant. Although growth of *crd1*Δ is not as defective as that of the *pgs1*Δ mutant, *crd1*Δ cells cannot form colonies at elevated temperatures from single cells plated on YPD media (Jiang *et al*., 1999; Zhong *et al*., 2004). At 36°C, only very tiny colonies of *crd1*Δ cells were visible on YPD plates, and cells from these colonies exhibited enlarged cell morphology (Figure 1). Interestingly, isogenic *CRD1 rho*° (WT *rho*°) cells did not display defective colony formation or aberrant cell morphology (Figure 1), suggesting that temperature sensitivity of *crd1*Δ is not due to defective mitochondrial bioenergetics. Although supplementation with sorbitol does rescue phenotypes of *crd1*Δ, *crd1*Δ cells do not exhibit cell wall defects (Zhong *et al*., 2007). However, rescue of *crd1*Δ by high osmolarity suggested that the mutant may have vacuolar defects.

To determine whether the enlarged cell morphology is due to aberrant vacuole volume, we examined vacuolar morphology using FM4-64, a lipophilic fluorescent dye that is transported into cells via the endocytic pathway and

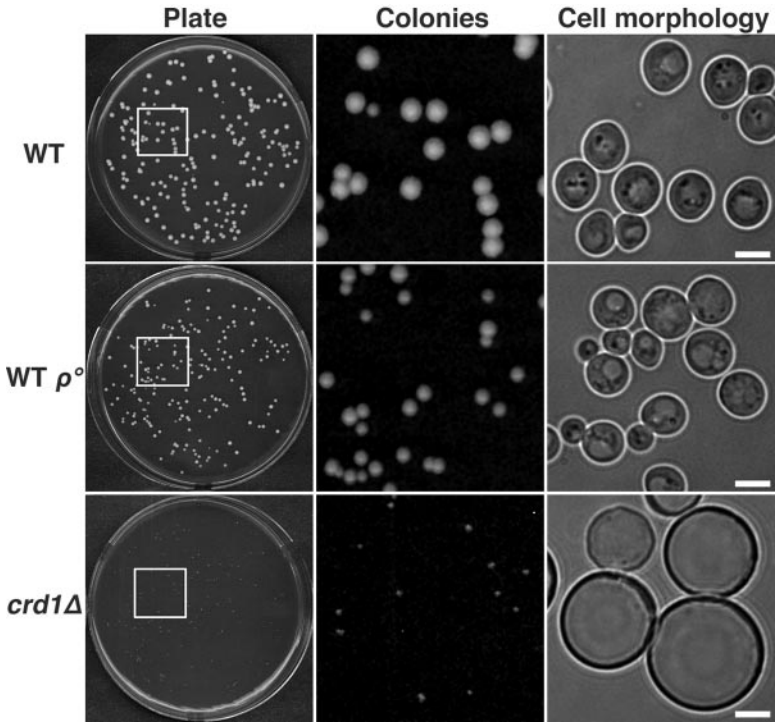

Figure 1. Loss of CL leads to defective colony formation and swollen cell size at elevated temperature. Yeast cells were grown in YPD media to the early stationary phase. Cells were seeded on YPD plates and incubated at 36°C. Colony and cell morphology were examined after 3–5 d of incubation. All images of cell morphology were taken at the same magnification (1000×). Bar, 2 μm.

ultimately accumulates in vacuolar membranes (Vida and Emr, 1995). A multilobed vacuole was observed in both WT and *crd1*Δ cells at optimal temperatures (Figure 2). However, at 37°C, the *crd1*Δ cells contained a single unlobed vacuole that was extremely swollen and composed the majority of the cell volume (Figure 2). The enlarged vacuole indicated that *crd1*Δ may be subject to defective vacuole membrane fission, thus losing osmoregulatory capabilities at high temperature.

Normally, the vacuole maintains a lower internal pH than that of the cytoplasm, and the acidic state of the vacuole plays a critical role in normal cellular functions (Mellman *et al.*, 1986; Kane, 2006). We used staining with quinacrine, a fluorescent weak base that diffuses across membranes and accumulates in acidic compartments (Weisman *et al.*, 1987), to determine whether *crd1*Δ cells were defective in vacuolar acidification. At 30°C, vacuoles in WT and *crd1*Δ cells were easily visualized by quinacrine staining. However, at 37°C, quinacrine fluorescence in *crd1*Δ is absent (Figure 2), indicative of a loss of vacuolar acidification. WT *rho*° cells did not display defective FM4-64 and quinacrine staining (Figure 2). Defects in colony formation, vacuolar morphology, and vacuolar acidification were all alleviated by supplementation with 1 M sorbitol (Figure 3). These data are consistent with the hypothesis that temperature sensitivity in *crd1*Δ results from abnormal biogenesis and/or acidification of the vacuole at high temperature.

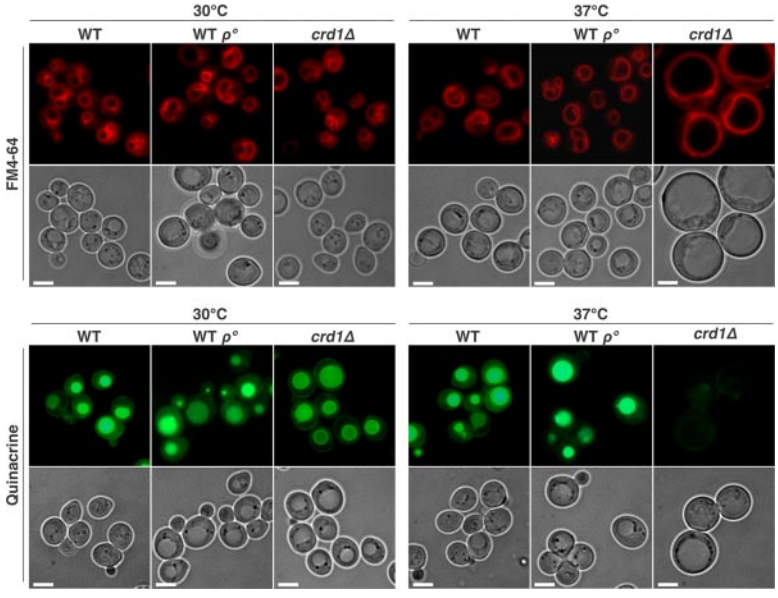

Figure 2. The *crd1*Δ mutant exhibits vacuolar defects at elevated temperature. Cells were grown to the mid-log phase in liquid YPD at 30°C or 37°C. Vacuoles were visualized by staining with FM4-64 or quinacrine. All images were taken at the same magnification (1000×). Bar, 2 μm.

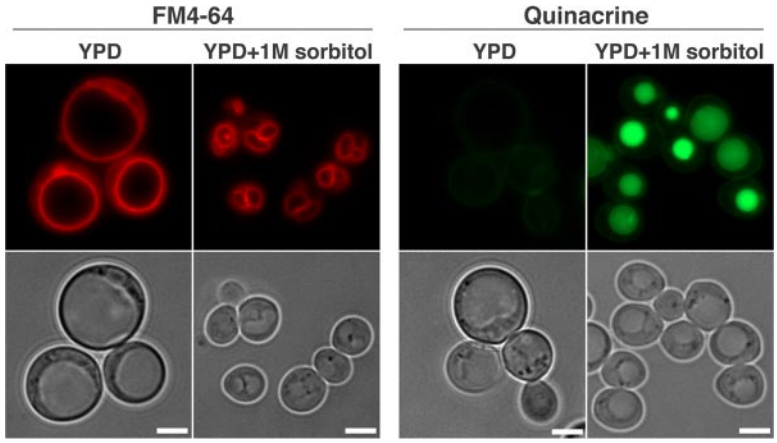

Figure 3. Vacuolar defects in *crd1*Δ are rescued by supplementation with 1 M sorbitol. Cells were grown to the mid-log phase in YPD or YPDS at 37°C. Vacuoles were visualized by staining with FM4-64 or quinacrine. All images were taken at the same magnification (1000×). Bar, 2 μm.

The crd1Δ Mutant Exhibits Decreased V-ATPase Activity at Elevated Temperature

The acidic pH of the yeast vacuolar lumen is generated by the V-ATPase, which carries out the active transport of protons across the membrane tightly coupled to the hydrolysis of ATP (Graham *et al*., 2003; Kane, 2006). We wanted to determine whether decreased vacuolar acidification in *crd1*Δ was due to defective V-ATPase activity. Vacuolar vesicles isolated from wild-type and *crd1*Δ mutants grown at 30°C contained similar levels of ATPase activity (Figure 4A), and *crd1*Δ vesicles did not exhibit defective proton pumping (Figure 4B), consistent with normal vacuolar function under these conditions. (In fact, vacuolar vesicles isolated from the crd1Δ mutant grown at 30°C showed somewhat better proton pumping than wild-type vesicles in two independent experiments.) However, vacuolar vesicles isolated from the *crd1*Δ mutant after a 3.5-h incubation at 37°C exhibited both decreased V-ATPase activity and proton pumping (Figure 4, A and B). Interestingly, the *crd1*Δ mutant did not exhibit low levels of V_0 a, V_1 A, and V_1 B subunits or vacuolar ALP (Figure 4C), suggesting that the observed decrease in V-ATPase activity and proton pumping in response to CL deficiency did not result from reduced levels of peripheral and membrane subunits of the V-ATPase. In addition, there was no obvious difference in levels of ALP between the vacuolar vesicles, suggesting that the vacuolar vesicles isolated were of comparable purity, despite differences in vacuolar morphology among the strains.

We speculated that the mechanism underlying vacuolar defects in response to decreased CL may be associated with some aspect of mitochondrial function, which is perturbed in CL mutants. Temperature sensitivity and vacuolar defects in *crd1*Δ cells are probably not due to mitochondrial respiratory dysfunction, because WT *rho*° cells did not exhibit these defects (Figures 1 and 2). Therefore, we hypothesized that the loss of CL may lead to defective metabolic reactions in mitochondria, which, in turn, trigger a pathway from the mitochondria to the vacuole. We addressed the possibility that the mitochondrial retrograde pathway mediated the effects on the vacuole in *crd1*Δ cells. In this pathway, the signaling protein Rtg2p senses mitochondrial dysfunction and transmits this signal to the transcriptional activators Rtg1p/Rtg3p, which translocate from the cytoplasm to the nucleus and activate transcription of target genes whose products replenish deficient mitochondrial components (Butow and Avadhani, 2004; Liu and Butow, 2006). To test the possibility that an overactive retrograde pathway could account for the vacuolar defects in *crd1*Δ cells, we determined the effects of disruption of *RTG2* on mutant. As seen in Figure 5A, the *crd1*Δ*rtg2*Δ double mutant formed colonies on YPD at 37°C and exhibited normal multilobed vacuole morphology and vacuolar acidification (Figure 6). Furthermore, deletion of *RTG2* enhanced V-ATPase activity and proton pumping in vacuolar vesicles isolated from *crd1*Δ at high temperature (Figure 4, A and B). Consistent with increased activity of Rtg2p in *crd1*Δ cells, the mRNA levels of *RTG2* were sixfold higher in *crd1*Δ than in WT cells (Figure 5B). Interestingly, supplementation with 1 M sorbitol reversed the increase in expression of *RTG2* (Figure 5C). However, increased *RTG2* in *crd1*Δ cells did not lead to a significant change in expression of the retrograde pathway target genes *CIT2* and *DLD3* (Figure 5, D and E), and deletion of *RTG3* in *crd1*Δ did not rescue temperature sensitivity (Figure 5A) or vacuolar defects (Figure 6), suggesting that mitochondrial retrograde regulation does not mediate the defective phenotypes in *crd1*Δ. Together, these findings suggest that Rtg2p mediates the vacuolar response to CL deficiency by a mechanism that seems to be independent of retrograde regulation.

Deletion of NHX1 Suppresses Vacuolar Defects and Temperature Sensitivity of crd1Δ

As shown above, the *crd1*Δ mutant exhibits loss of vacuolar acidification due to decreased coupling of V-ATPase activity and proton pumping. However, acidification defects alone cannot explain the aberrant vacuolar morphology seen in the *crd1*Δ mutant, because V-ATPase mutants do not exhibit similar morphological defects (Wickner and Haas, 2000; Weisman, 2003). Thus, we wanted to determine the mechanism leading to defective vacuolar morphology in *crd1*Δ. The enlarged vacuolar morphology in the *crd1*Δ mutant is consistent with a loss of osmoregulatory capabilities and defective ion homeostasis. We hypothesized that perturbation of ion pumps that mediate vacuolar ion homeostasis may thus suppress vacuolar defects in *crd1*Δ. To this end, we constructed double mutants of *crd1*Δ and *vcx1*Δ, *pmc1*Δ, *yvc1*Δ, *nhx1*Δ and *cch1*Δ and examined vacuolar defects in the double mutants. Deletion of *NHX1*, but not deletion of the other pump genes, rescued both vacuolar defects and defective colony formation (Figure 7). Quinacrine fluorescence was easily visualized in *crd1*Δ*nhx1*Δ, consistent with restoration of vacuolar acidification. *NHX1* encodes a Na^+/H^+ exchanger localized in the membranes of the late endosomal/prevacuolar compartment where it mediates osmotolerance and intracellular sequestration of Na^+ in a pH-dependent manner (Nass *et al*., 1997; Nass and Rao,

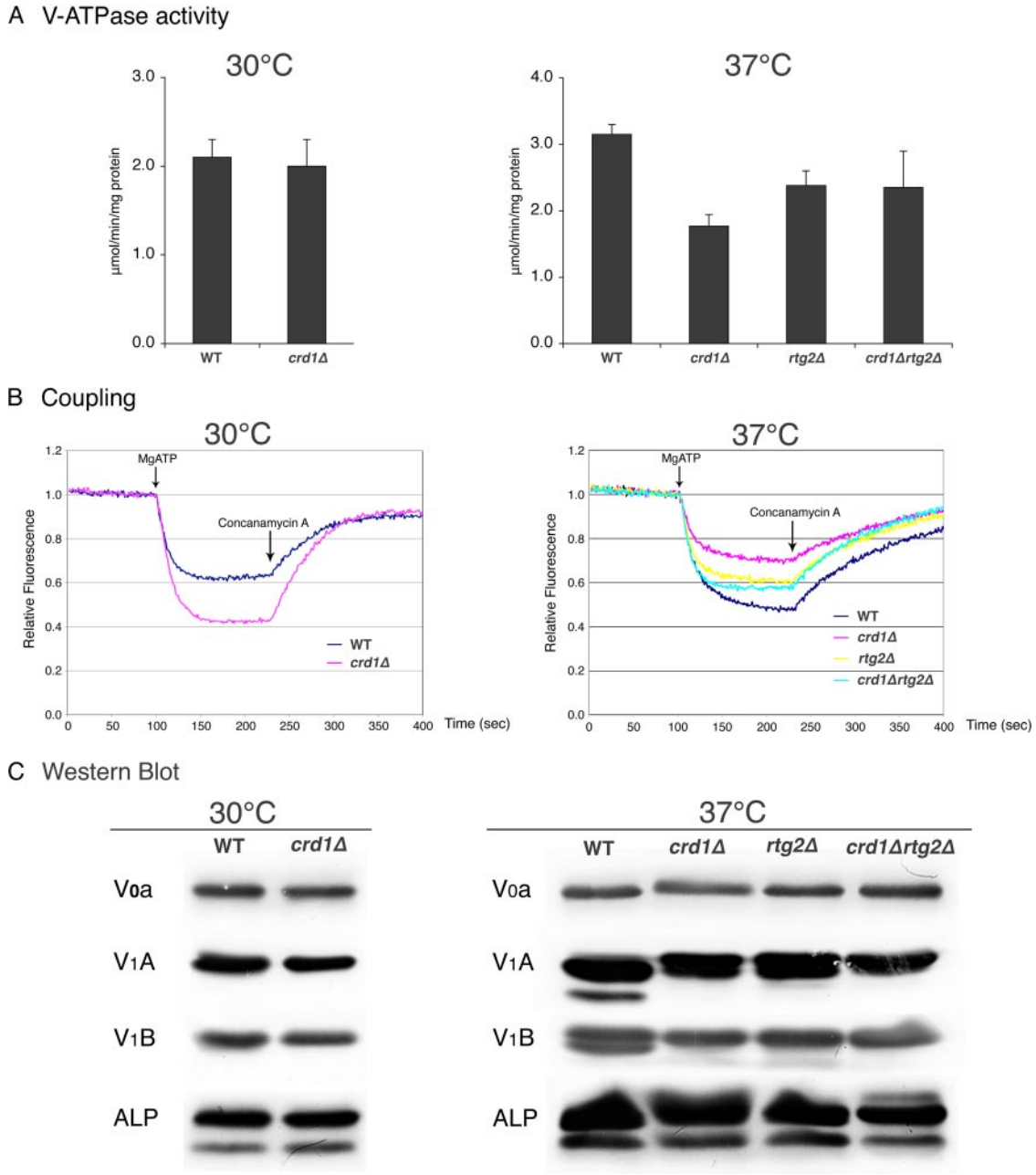

Figure 4. Deletion of *RTG2* rescues V-ATPase defects in *crd1*Δ at elevated temperature. Vacuolar vesicles were isolated from the indicated mutants grown to early log phase in YPD at 30°C with (37°C) or without (30°C) a shift to 37°C for 3.5 h as described in *Materials and Methods*. (A) The average V-ATPase activity from two independent preparations of vesicles is shown. Error bars represent the range of the two preparations. (B) Proton pumping was assayed in vacuolar vesicles from each strain by monitoring ACMA fluorescence quenching. Vesicles (20 μg/assay) were equilibrated in ACMA, and pumping was initiated by addition of MgATP (0.5 mM ATP and 1 mM $MgSO_4$). Quenching was reversed by addition of concanamycin A to a final concentration of 100 nM. A representative assay for each condition is shown. (C) Levels of V-ATPase subunits V_1 A and B and V_0 a, as well as the vacuolar membrane protein ALP, in the various vacuolar vesicles preparations were visualized by immunoblotting as described in *Materials and Methods*. Equivalent amounts of vacuolar protein (5 μg for visualization of V_1 A and V_1 B and 10 μg for visualization of V_0 a and ALP) were loaded for each strain and temperature.

1998, 1999). In addition, Nhx1p regulates vacuolar pH by transporting H^+ in a direction opposite to that of the V-ATPase (Brett *et al.*, 2005). Therefore, disruption of *NHX1* may compensate for loss of vacuolar acidification in a *crd1*Δ mutant by reducing the loss of protons from the vacuole (Brett *et al.*, 2005; Mukherjee *et al.*, 2006).

The vacuoles of the *nhx1*Δ and *crd1*Δ*nhx1*Δ mutants were weakly stained with FM4-64 (Figure 7), consistent with previous reports that the loss of Nhx1p leads to decreased vacuolar staining with this dye (Bowers *et al.*, 2000; Brett *et al.*, 2005). The vacuolar morphology of the *crd1*Δ*nhx1*Δ double mutant was similar to that of wild type, indicating that *nhx1*Δ suppressed the swollen vacuole morphology of the *crd1*Δ mutant. These results suggested that, in addition to a defective V-ATPase, *crd1*Δ exhibits aberrant vacuolar ion homeostasis. One possible explanation for restoration of

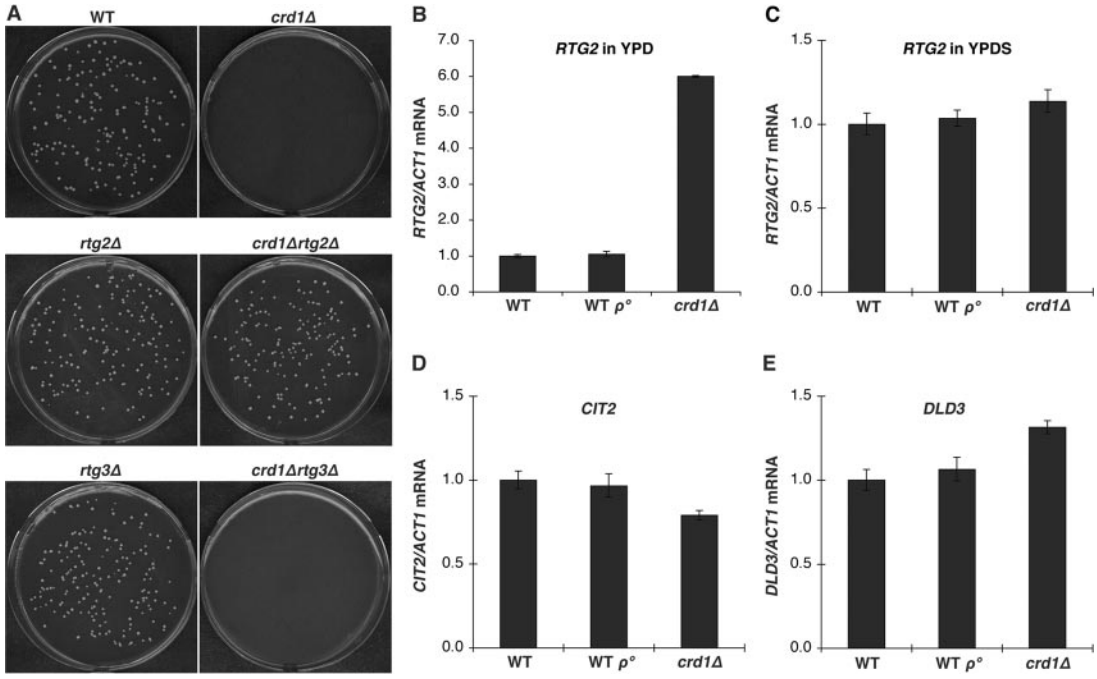

Figure 5. Deletion of *RTG2* suppresses defective colony formation in *crd1*Δ at elevated temperature. (A) Yeast cells were grown in YPD media to the early stationary phase. Cells were seeded on YPD plates and incubated at 37°C for 3–5 d. (B–E) Total RNA was extracted from cells grown to the mid-log phase in YPD or YPDS at 37°C, and mRNA levels were determined by quantitative real-time PCR analysis. Expression was normalized to the mRNA levels of the internal control *ACT1*. Error bars represent the range of the three independent experiments.

wild-type vacuolar morphology by *nhx1*Δ is that the enlarged vacuole in *crd1*Δ could be attributed to excessive influx of Na^+ through Nhx1p and an accompanying influx of water. Calcineurin, a Ca^{2+}-dependent target of calmodulin (Cyert, 2003; Kraus and Heitman, 2003), plays a key role in adaptation to Na^+ stress by inducing the transition of a K^+/Na^+ uptake system at the plasma membrane to restrict influx of Na^+ (Mendoza *et al*., 1996), and by promoting the expression of *ENA1*, a gene encoding a P-type ATPase Na^+ pump that mediates Na^+ efflux (Nakamura *et al*., 1993; Mendoza *et al*., 1994). Calcineurin expression and activity are increased in response to internal Na^+ stress (Mendoza *et al*., 1996). Interestingly, the *crd1*Δ mutant exhibited increased expression of the genes encoding calmodulin (*CMD1*) as well as the catalytic (*CNA1* and *CNA2*) and regulatory (*CNB1*) subunits of calcineurin (Figure 8, A–D). *CNA1* and *CNB1* exhibited the greatest increases in expression at 5.6- and 12-fold, respectively (Figure 8, B and D). These findings

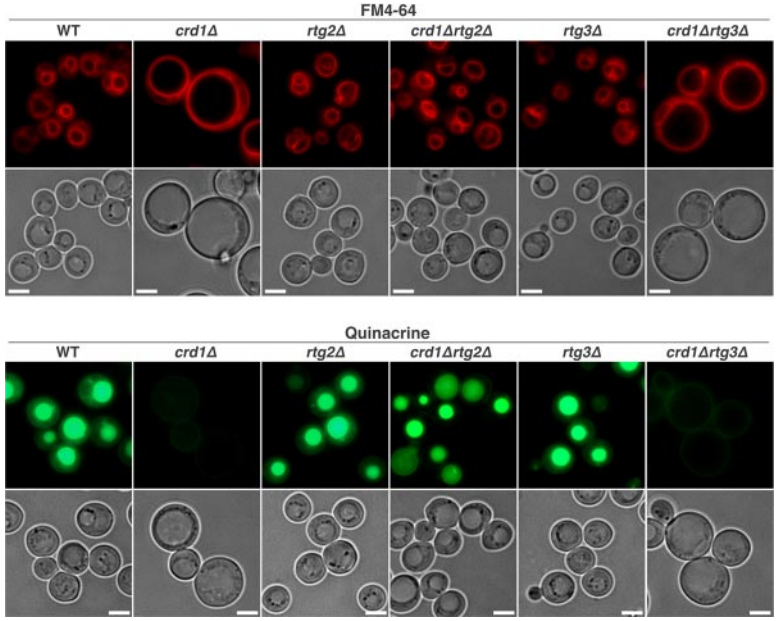

Figure 6. Deletion of *RTG2* rescues vacuolar defects in *crd1*Δ at elevated temperature. Cells were grown to the mid-log phase in liquid YPD at 37°C. Vacuoles were visualized by staining with FM4-64 or quinacrine. All images were taken at the same magnification (1000×). Bar, 2 μm.

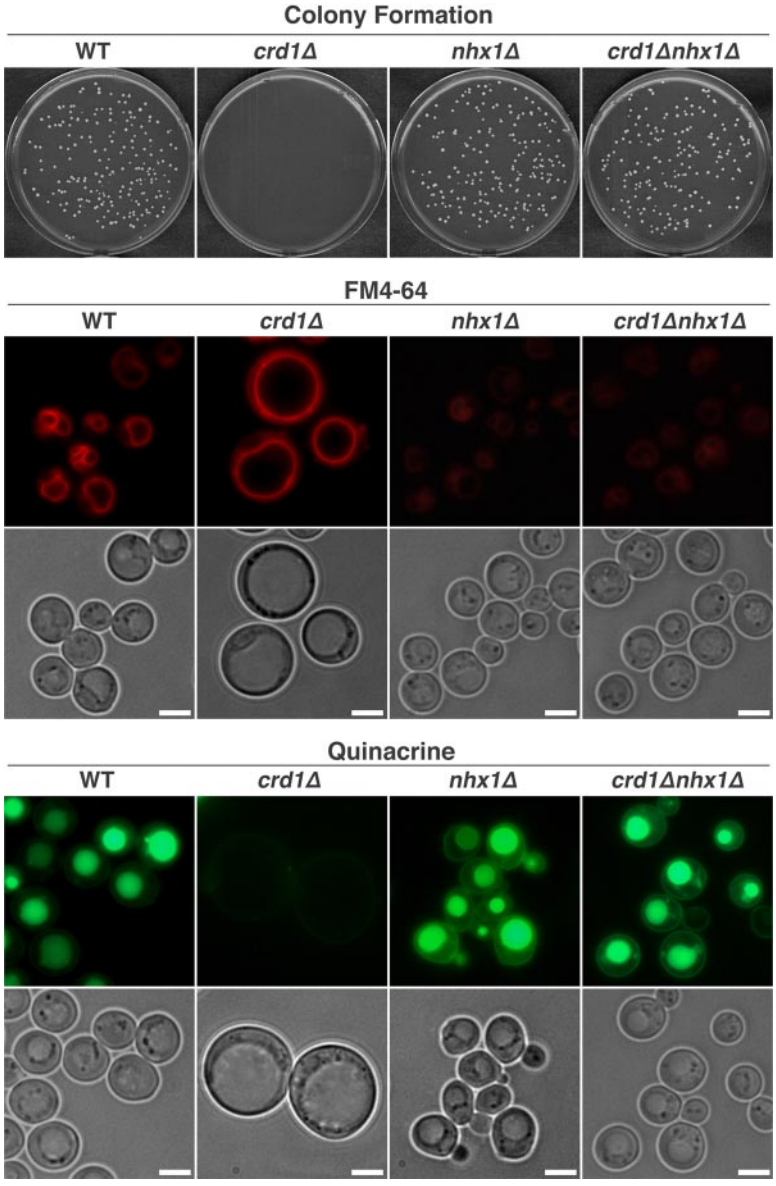

Figure 7. Deletion of *NHX1* suppresses colony formation and vacuolar defects in *crd1*Δ at elevated temperature. Colony formation was determined as in the legend to Figure 1. Vacuolar acidification and morphology were determined as described in *Materials and Methods*, and all images were taken at the same magnification (1000×). Bar, 2 μm.

suggest that increased calcineurin expression in response to Na^+ stress in *crd1*Δ is required for alleviation of growth defects. Consistent with this, deletion of *CNB1* exacerbated the temperature sensitivity of *crd1*Δ. Thus, although *crd1*Δ cells could form colonies at 35°C, the double mutant *crd1*Δ*cnb1*Δ could not (Figure 8E). These findings suggest that up-regulation of expression of calcineurin (and/or calmodulin) genes may be compensatory feedback to attenuate the putative intracellular ion stress in *crd1*Δ.

DISCUSSION

In this study, we addressed the hypothesis that the loss of CL in the *crd1*Δ mutant leads to defective colony formation at elevated temperature due to vacuolar defects. Consistent with this hypothesis, the *crd1*Δ mutant exhibited swollen vacuole morphology, loss of vacuolar acidification, and decreases in V-ATPase activity and proton pumping in isolated vacuoles. Similarly, swollen vacuole morphology and loss of vacuolar acidification also could be observed in *pgs1*Δ (Supplemental Figure S1), which supports the connection between CL deficiency and vacuolar defects. It is likely that the signaling protein Rtg2p mediates the vacuolar response to CL deficiency, as deletion of *RTG2* suppresses vacuolar and growth defects in the *crd1*Δ mutant. The mechanism underlying these defects seems to involve perturbation of ion homeostasis, because growth and vacuolar defects could also be suppressed by deletion of the Na^+/H^+ exchanger *NHX1*. These results indicate that CL is required for processes that are essential for normal vacuolar function, suggesting that CL-mediated cross-talk exists between the mitochondria and the vacuole.

The finding that *rtg2*Δ suppresses the colony formation defect of *crd1*Δ provides a clue to the mechanism underlying mitochondria–vacuole cross-talk. Attenuation of defective vacuolar acidification and abnormal morphology by disruption of *RTG2* (Figure 6) suggests that Rtg2p is involved in mediation of vacuole function. Suppression is most likely not associated with mitochondrial retrograde regulation, because deletion of *RTG3*, which transduces the retrograde

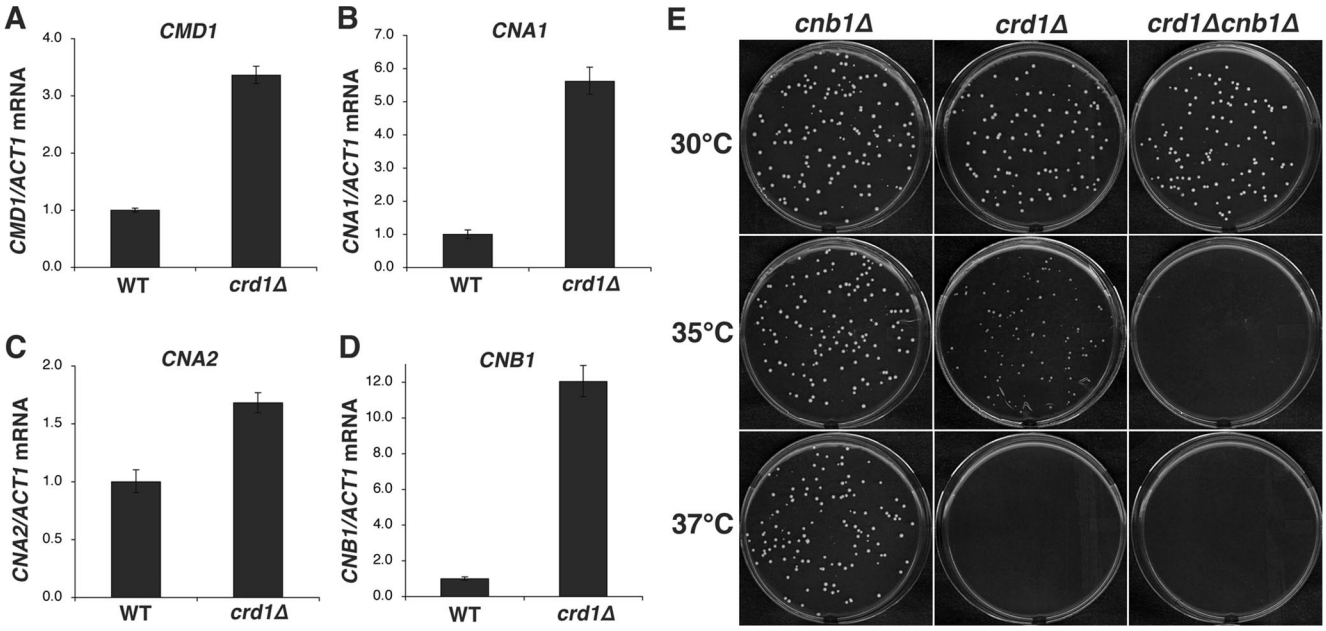

Figure 8. The *crd1*Δ*cnb1*Δ mutant exhibits defective colony formation at 35°C. (A–D) Total RNA was extracted from cells grown to the mid-log phase in YPD at 37°C. mRNA levels were determined by quantitative real-time PCR. Expression was normalized to the mRNA levels of the internal control *ACT1*. Error bars represent the range of the three independent experiments. (E) Yeast cells were grown in YPD media to the early stationary phase. Cells were seeded on YPD plates and incubated at the indicated temperature for 3–5 d.

signal (Butow and Avadhani, 2004; Liu and Butow, 2006), does not suppress vacuolar defects (Figure 6). Rather, the high expression of *RTG2* itself may contribute to vacuolar dysfunction. However, it is unlikely that increased Rtg2p alone affects the vacuole in the absence of mitochondrial dysfunction, because we have observed that overexpression of *RTG2* in wild-type cells does not cause vacuolar defects (Supplemental Figure S2). Rtg2p is a critical sensor of mitochondrial dysfunction and also functions as an essential component of the SLIK (Spt-Ada-Gcn5-acetytransferase-like) histone acetyltransferase (HAT) complex (Pray-Grant *et al*., 2002). Elevated expression of *RTG2* in response to mitochondrial dysfunction in the CL mutant may stabilize the HAT complex, resulting in altered expression of genes affecting V-ATPase activity and proton pump coupling, although immunoblots of vacuolar membranes indicated near-normal levels of several peripheral and membrane subunits of the V-ATPase (Figure 4C). Alternatively, the possibility that Rtg2p directly transmits signals or affects the V-ATPase cannot be ruled out.

The presence of an enlarged vacuole accompanied by swollen cell size in *crd1*Δ is consistent with an osmotic imbalance. However, it is unlikely that these defects are a direct consequence of perturbed vacuolar acidification in *crd1*Δ, because vacuolar membrane ATPase (*vma*) mutants do not have these phenotypes (Wickner and Haas, 2000; Weisman, 2003). Furthermore, although *crd1*Δ exhibits defective V-ATPase activity, it does not have characteristic *vma* phenotypes (Nelson and Nelson, 1990; Ohya *et al*., 1991). Specifically, the *crd1*Δ mutant is not sensitive to high calcium concentrations, and the growth defect of *crd1*Δ cannot be rescued in medium buffered to pH 5 (Supplemental Figure S3). More likely, the vacuolar morphology defect in *crd1*Δ may be due to perturbation of ion homeostasis, because *nhx1*Δ suppresses vacuolar defects in the mutant (Figure 7). Suppression of *crd1*Δ phenotypes by *nhx1*Δ suggests that *crd1*Δ is subject to defective vacuolar ion homeostasis most likely due to excessive ion influx, accompanied by a compensatory influx of water. One likely explanation is that mitochondria may be involved in regulating cellular ion levels. In the absence of CL, yeast cells are subject to excessive cellular ion influx. In response, Nhx1p sequesters more ions (Na^+ and K^+) and swells the vacuole. Disruption of *NHX1* in *crd1*Δ may prevent the vacuole from being engorged with an excess of ions and water, thus avoiding collapse of the vacuolar proton gradient due to proton depletion. By pumping out H^+ coupled with Na^+ influx, Nhx1p serves to alkalinize the endosomal and vacuolar lumen (Hirata *et al*., 2002). Thus, both V-ATPase and Nhx1p participate in normal pH homeostasis.

Calcineurin plays a critical role in responding to Na^+ stress (Yoshimoto *et al*., 2002). The calcineurin mutant *cnb1* exhibits defects in down-regulating intracellular Na^+ levels and is sensitive to Na^+ stress, but not to K^+, Ca^{2+} or Mg^{2+} (Nakamura *et al*., 1993; Mendoza *et al*., 1994). Consistent with this, overexpression of calcineurin mimics a Na^+ stress signal (Mendoza *et al*., 1996). Therefore, increased expression of genes encoding calcineurin (*CNA1*, *CNA2*, and *CNB1*) in *crd1*Δ is most likely an indication of intracellular Na^+ stress. As calcineurin is reported to control sodium homeostasis by both promoting Na^+ efflux and repressing Na^+ influx (Mendoza *et al*., 1996), increased *CNA1*, *CNA2*, and *CNB1* expression may be feedback compensation in response to the putative internal Na^+ stress in *crd1*Δ. In addition, calcineurin inhibits *VCX1*-dependent H^+/Ca^{2+} exchange that may contribute to vacuolar defects in *crd1*Δ. The exacerbation of defective colony formation of *crd1*Δ by *cnb1*Δ suggests that increased expression of calcineurin genes is required for alleviating ion stress in *crd1*Δ at elevated temperature. However, increased calcineurin expression is not sufficient to attenuate excessive cellular and vacuolar uptake of ions, which can be brought about by deletion of *NHX1*. Interestingly, *cnb1* and *vma* mutants are synthetically lethal (Garrett-Engele *et al*., 1995; Tanida *et al*., 1995),

which underscores the important role of calcineurin and V-ATPase in Ca^{2+} homeostasis (Tanida *et al*., 1995; Forster and Kane, 2000). It is possible that the exacerbation of defective growth of *crd1*Δ*cnb1*Δ is due in part to defective Ca^{2+} homeostasis, although *crd1*Δ does not lose V-ATPase activity completely.

The mechanism whereby 1 M sorbitol restores vacuolar acidification in *crd1*Δ is not clear. A clue to this mechanism may derive from the fact that phenotypes in *crd1*Δ resemble those of mutants of *FAB1*, which encodes a lipid kinase that converts phosphatidylinositol 3-phosphate (PtdIns3P) to phosphatidylinositol 3,5-bisphosphate [PtdIns(3,5)P_2]. PtdIns(3,5)P_2 plays an important role in cellular adaptation to extracellular osmolarity (Cooke *et al*., 1998). The levels of PtdIns(3,5)P_2 rise dramatically in response to osmotic stress, signaling a protective response (Dove *et al*., 1997; Bonangelino *et al*., 2002). Basal levels of PtdIns(3,5)P_2 are essential for maintenance of vacuolar morphology and acidification (Efe *et al*., 2005). Hyperosmotic stress causes shrunken and fragmented vacuoles due to increased PtdIns(3,5)P_2 synthesis (Bonangelino *et al*., 2002). In the *fab1* mutant, PtdIns(3,5)P_2 is not detectable in vivo, and cells display pleiotropic phenotypes similar to those of the *crd1*Δ mutant, including a dramatically enlarged vacuole, loss of vacuolar acidification and decreased growth at high temperature, phenotypes that are not restored by increased osmolarity (Yamamoto *et al*., 1995; Gary *et al*., 1998) (Bonangelino *et al*., 2002). Thus, it is tempting to speculate that the mutant phenotypes of *crd1*Δ are due to defective PtdIns(3,5)P_2 synthesis, which is restored by 1 M sorbitol. Arguing against this possibility is the observation that expression of *FAB1* pathway genes, including *FAB1*, *VAC7*, *VAC14*, *VPS15*, *VPS34*, *FIG4*, and *ATG18* is not altered in *crd1*Δ (Supplemental Figure S4). However, much of the regulation of these proteins is posttranslational, so altered activity of the *FAB1* pathway cannot be ruled out.

In summary, we demonstrate for the first time that the absence of CL leads to severe vacuolar defects at elevated temperature. The yeast vacuole is analogous to the mammalian lysosome and plays an important role in ion and water homeostasis, storage of phosphate and amino acids, and protein turnover (Klionsky *et al*., 1990; Wickner and Haas, 2000; Weisman, 2003). Rapid changes in shape, volume, and number of vacuoles are critical to ensure an immediate response to environmental variation (Klionsky *et al*., 1990; Latterich and Watson, 1993). The establishment and maintenance of vacuolar acidification are achieved by the V-ATPase, which is required for optimal proteolytic activation, protein sorting and ion homeostasis (Graham *et al*., 2003; Kane, 2006). Impaired V-ATPase activity and misregulation of ion homeostasis in *crd1*Δ indicate that a novel mitochondria-vacuole signaling pathway is mediated by the synthesis of CL. Our findings expand the understanding of essential cellular functions of CL and point to a regulatory role of mitochondria in vacuolar functions.

ACKNOWLEDGMENTS

We thank Quan He, Quan Zhong, Guiling Li, Jingming Zhou, Amit Joshi, Rania Deranieh and Morgan Thompson for helpful advice. This work was supported by a grant from the Barth Syndrome Foundation to M.L.G. and by National Institutes of Health grants HL-62263 (to M.L.G.) and GM-50322 (to P.M.K.).

REFERENCES

Ali, R., Brett, C. L., Mukherjee, S., and Rao, R. (2004). Inhibition of sodium/proton exchange by a Rab-GTPase-activating protein regulates endosomal traffic in yeast. J. Biol. Chem. *279*, 4498–4506.

Beyer, K., and Nuscher, B. (1996). Specific cardiolipin binding interferes with labeling of sulfhydryl residues in the adenosine diphosphate/adenosine triphosphate carrier protein from beef heart mitochondria. Biochemistry *35*, 15784–15790.

Blomberg, A. (1995). Global changes in protein synthesis during adaptation of the yeast *Saccharomyces cerevisiae* to 0.7 M NaCl. J. Bacteriol. *177*, 3563–3572.

Bonangelino, C. J., Nau, J. J., Duex, J. E., Brinkman, M., Wurmser, A. E., Gary, J. D., Emr, S. D., and Weisman, L. S. (2002). Osmotic stress-induced increase of phosphatidylinositol 3,5-bisphosphate requires Vac14p, an activator of the lipid kinase Fab1p. J. Cell Biol. *156*, 1015–1028.

Bowers, K., Levi, B. P., Patel, F. I., and Stevens, T. H. (2000). The sodium/proton exchanger Nhx1p is required for endosomal protein trafficking in the yeast *Saccharomyces cerevisiae*. Mol. Biol. Cell *11*, 4277–4294.

Brett, C. L., Tukaye, D. N., Mukherjee, S., and Rao, R. (2005). The yeast endosomal Na+K+/H+ exchanger Nhx1 regulates cellular pH to control vesicle trafficking. Mol. Biol. Cell *16*, 1396–1405.

Butow, R. A., and Avadhani, N. G. (2004). Mitochondrial signaling: the retrograde response. Mol. Cell *14*, 1–15.

Chang, S. C., Heacock, P. N., Clancey, C. J., and Dowhan, W. (1998a). The PEL1 gene (renamed PGS1) encodes the phosphatidylglycero-phosphate synthase of *Saccharomyces cerevisiae*. J. Biol. Chem. *273*, 9829–9836.

Chang, S. C., Heacock, P. N., Mileykovskaya, E., Voelker, D. R., and Dowhan, W. (1998b). Isolation and characterization of the gene (CLS1) encoding cardiolipin synthase in *Saccharomyces cerevisiae*. J. Biol. Chem. *273*, 14933–14941.

Chen, S., He, Q., and Greenberg, M. L. (2008). Loss of tafazzin in yeast leads to increased oxidative stress during respiratory growth. Mol. Microbiol. *68*, 1061–1072.

Cooke, F. T., Dove, S. K., McEwen, R. K., Painter, G., Holmes, A. B., Hall, M. N., Michell, R. H., and Parker, P. J. (1998). The stress-activated phosphatidylinositol 3-phosphate 5-kinase Fab1p is essential for vacuole function in *S. cerevisiae*. Curr. Biol. *8*, 1219–1222.

Cyert, M. S. (2003). Calcineurin signaling in *Saccharomyces cerevisiae*: how yeast go crazy in response to stress. Biochem. Biophys. Res. Commun. *311*, 1143–1150.

Daum, G. (1985). Lipids of mitochondria. Biochim. Biophys. Acta *822*, 1–42.

Dove, S. K., Cooke, F. T., Douglas, M. R., Sayers, L. G., Parker, P. J., and Michell, R. H. (1997). Osmotic stress activates phosphatidylinositol-3,5-bisphosphate synthesis. Nature *390*, 187–192.

Drees, M., and Beyer, K. (1988). Interaction of phospholipids with the detergent-solubilized ADP/ATP carrier protein as studied by spin-label electron spin resonance. Biochemistry *27*, 8584–8591.

Dzugasova, V., Obernauerova, M., Horvathova, K., Vachova, M., Zakova, M., and Subik, J. (1998). Phosphatidylglycerolphosphate synthase encoded by the PEL1/PGS1 gene in *Saccharomyces cerevisiae* is localized in mitochondria and its expression is regulated by phospholipid precursors. Curr. Genet. *34*, 297–302.

Efe, J. A., Botelho, R. J., and Emr, S. D. (2005). The Fab1 phosphatidylinositol kinase pathway in the regulation of vacuole morphology. Curr. Opin. Cell Biol. *17*, 402–408.

Forster, C., and Kane, P. M. (2000). Cytosolic Ca2+ homeostasis is a constitutive function of the V-ATPase in *Saccharomyces cerevisiae*. J. Biol. Chem. *275*, 38245–38253.

Garrett-Engele, P., Moilanen, B., and Cyert, M. S. (1995). Calcineurin, the Ca2+/calmodulin-dependent protein phosphatase, is essential in yeast mutants with cell integrity defects and in mutants that lack a functional vacuolar H(+)-ATPase. Mol. Cell. Biol. *15*, 4103–4114.

Gary, J. D., Wurmser, A. E., Bonangelino, C. J., Weisman, L. S., and Emr, S. D. (1998). Fab1p is essential for PtdIns(3)P 5-kinase activity and the maintenance of vacuolar size and membrane homeostasis. J. Cell Biol. *143*, 65–79.

Gomez, B., Jr., and Robinson, N. C. (1999). Phospholipase digestion of bound cardiolipin reversibly inactivates bovine cytochrome bc1. Biochemistry *38*, 9031–9038.

Graham, L. A., Flannery, A. R., and Stevens, T. H. (2003). Structure and assembly of the yeast V-ATPase. J. Bioenerg. Biomembr. *35*, 301–312.

Gu, Z., Gohil, V., Zhong, Q., Schlame, M., and Greenberg, M. L. (2002). The biosynthesis and remodeling of cardiolipin in lipids. Glycerolipid Metabolizing Enzyme, 67–84.

Gu, Z., Valianpour, F., Chen, S., Vaz, F. M., Hakkaart, G. A., Wanders, R. J., and Greenberg, M. L. (2004). Aberrant cardiolipin metabolism in the yeast taz1 mutant: a model for Barth syndrome. Mol. Microbiol. *51*, 149–158.

Hayer-Hartl, M., Schagger, H., von Jagow, G., and Beyer, K. (1992). Interactions of phospholipids with the mitochondrial cytochrome-c reductase studied by spin-label ESR and NMR spectroscopy. Eur. J. Biochem. *209*, 423–430.

Hirata, T., Wada, Y., and Futai, M. (2002). Sodium and sulfate ion transport in yeast vacuoles. J. Biochem. *131*, 261–265.

Hoch, F. L. (1992). Cardiolipins and biomembrane function. Biochim. Biophys. Acta *1113*, 71–133.

Hohmann, S. (2002). Osmotic stress signaling and osmoadaptation in yeasts. Microbiol. Mol. Biol. Rev. *66*, 300–372.

Janitor, M., and Subik, J. (1993). Molecular cloning of the PEL1 gene of *Saccharomyces cerevisiae* that is essential for the viability of petite mutants. Curr. Genet. *24*, 307–312.

Jiang, F., Gu, Z., Granger, J. M., and Greenberg, M. L. (1999). Cardiolipin synthase expression is essential for growth at elevated temperature and is regulated by factors affecting mitochondrial development. Mol. Microbiol. *31*, 373–379.

Jiang, F., Rizavi, H. S., and Greenberg, M. L. (1997). Cardiolipin is not essential for the growth of *Saccharomyces cerevisiae* on fermentable or non-fermentable carbon sources. Mol. Microbiol. *26*, 481–491.

Jiang, F., Ryan, M. T., Schlame, M., Zhao, M., Gu, Z., Klingenberg, M., Pfanner, N., and Greenberg, M. L. (2000). Absence of cardiolipin in the crd1 null mutant results in decreased mitochondrial membrane potential and reduced mitochondrial function. J. Biol. Chem. *275*, 22387–22394.

Kane, P. M. (2006). The where, when, and how of organelle acidification by the yeast vacuolar H+-ATPase. Microbiol. Mol. Biol. Rev. *70*, 177–191.

Kane, P. M., Kuehn, M. C., Howald-Stevenson, I., and Stevens, T. H. (1992). Assembly and targeting of peripheral and integral membrane subunits of the yeast vacuolar H(+)-ATPase. J. Biol. Chem. *267*, 447–454.

Klionsky, D. J., Herman, P. K., and Emr, S. D. (1990). The fungal vacuole: composition, function, and biogenesis. Microbiol. Rev. *54*, 266–292.

Koshkin, V., and Greenberg, M. L. (2000). Oxidative phosphorylation in cardiolipin-lacking yeast mitochondria. Biochem. J. 347, 687–691.

Koshkin, V., and Greenberg, M. L. (2002). Cardiolipin prevents rate-dependent uncoupling and provides osmotic stability in yeast mitochondria. Biochem. J. *364*, 317–322.

Kraus, P. R., and Heitman, J. (2003). Coping with stress: calmodulin and calcineurin in model and pathogenic fungi. Biochem. Biophys. Res. Commun. *311*, 1151–1157.

Latterich, M., and Watson, M. D. (1993). Evidence for a dual osmoregulatory mechanism in the yeast *Saccharomyces cerevisiae*. Biochem. Biophys. Res. Commun. *191*, 1111–1117.

Li, G., Chen, S., Thompson, M. N., and Greenberg, M. L. (2007). New insights into the regulation of cardiolipin biosynthesis in yeast: implications for Barth syndrome. Biochim. Biophys. Acta *1771*, 432–441.

Liu, M., Tarsio, M., Charsky, C. M., and Kane, P. M. (2005). Structural and functional separation of the N- and C-terminal domains of the yeast V-ATPase subunit H. J. Biol. Chem. *280*, 36978–36985.

Liu, Z., and Butow, R. A. (2006). Mitochondrial retrograde signaling. Annu. Rev. Genet. *40*, 159–185.

Ma, L., Vaz, F. M., Gu, Z., Wanders, R. J., and Greenberg, M. L. (2004). The human TAZ gene complements mitochondrial dysfunction in the yeast taz1Delta mutant. Implications for Barth syndrome. J. Biol. Chem. *279*, 44394–44399.

Mellman, I., Fuchs, R., and Helenius, A. (1986). Acidification of the endocytic and exocytic pathways. Annu. Rev. Biochem. *55*, 663–700.

Mendoza, I., Quintero, F. J., Bressan, R. A., Hasegawa, P. M., and Pardo, J. M. (1996). Activated calcineurin confers high tolerance to ion stress and alters the budding pattern and cell morphology of yeast cells. J. Biol. Chem. *271*, 23061–23067.

Mendoza, I., Rubio, F., Rodriguez-Navarro, A., and Pardo, J. M. (1994). The protein phosphatase calcineurin is essential for NaCl tolerance of *Saccharomyces cerevisiae*. J. Biol. Chem. *269*, 8792–8796.

Mukherjee, S., Kallay, L., Brett, C. L., and Rao, R. (2006). Mutational analysis of the intramembranous H10 loop of yeast Nhx1 reveals a critical role in ion homoeostasis and vesicle trafficking. Biochem. J. *398*, 97–105.

Nakamura, T., Liu, Y., Hirata, D., Namba, H., Harada, S., Hirokawa, T., and Miyakawa, T. (1993). Protein phosphatase type 2B (calcineurin)-mediated, FK506-sensitive regulation of intracellular ions in yeast is an important determinant for adaptation to high salt stress conditions. EMBO J. *12*, 4063–4071.

Nass, R., Cunningham, K. W., and Rao, R. (1997). Intracellular sequestration of sodium by a novel Na+/H+ exchanger in yeast is enhanced by mutations in the plasma membrane H+-ATPase. Insights into mechanisms of sodium tolerance. J. Biol. Chem. *272*, 26145–26152.

Nass, R., and Rao, R. (1998). Novel localization of a Na+/H+ exchanger in a late endosomal compartment of yeast. Implications for vacuole biogenesis. J. Biol. Chem. *273*, 21054–21060.

Nass, R., and Rao, R. (1999). The yeast endosomal Na+/H+ exchanger, Nhx1, confers osmotolerance following acute hypertonic shock. Microbiology *145*, 3221–3228.

Nelson, H., and Nelson, N. (1990). Disruption of genes encoding subunits of yeast vacuolar H(+)-ATPase causes conditional lethality. Proc. Natl. Acad. Sci. USA *87*, 3503–3507.

Norbeck, J., and Blomberg, A. (1996). Protein expression during exponential growth in 0.7 M NaCl medium of *Saccharomyces cerevisiae*. FEMS Microbiol. Lett. *137*, 1–8.

Ohya, Y., Umemoto, N., Tanida, I., Ohta, A., Iida, H., and Anraku, Y. (1991). Calcium-sensitive cls mutants of *Saccharomyces cerevisiae* showing a Pet-phenotype are ascribable to defects of vacuolar membrane H(+)-ATPase activity. J. Biol. Chem. *266*, 13971–13977.

Pfeiffer, K., Gohil, V., Stuart, R. A., Hunte, C., Brandt, U., Greenberg, M. L., and Schagger, H. (2003). Cardiolipin stabilizes respiratory chain supercomplexes. J. Biol. Chem. *278*, 52873–52880.

Posas, F., Chambers, J. R., Heyman, J. A., Hoeffler, J. P., de Nadal, E., and Arino, J. (2000). The transcriptional response of yeast to saline stress. J. Biol. Chem. *275*, 17249–17255.

Pray-Grant, M. G., Schieltz, D., McMahon, S. J., Wood, J. M., Kennedy, E. L., Cook, R. G., Workman, J. L., Yates, J. R., 3rd, and Grant, P. A. (2002). The novel SLIK histone acetyltransferase complex functions in the yeast retrograde response pathway. Mol. Cell. Biol. *22*, 8774–8786.

Rep, M., Krantz, M., Thevelein, J. M., and Hohmann, S. (2000). The transcriptional response of *Saccharomyces cerevisiae* to osmotic shock. Hot1p and Msn2p/Msn4p are required for the induction of subsets of high osmolarity glycerol pathway-dependent genes. J. Biol. Chem. *275*, 8290–8300.

Roberts, C. J., Raymond, C. K., Yamashiro, C. T., and Stevens, T. H. (1991). Methods for studying the yeast vacuole. Methods Enzymol. *194*, 644–661.

Robinson, N. C., Zborowski, J., and Talbert, L. H. (1990). Cardiolipin-depleted bovine heart cytochrome c oxidase: binding stoichiometry and affinity for cardiolipin derivatives. Biochemistry *29*, 8962–8969.

Schlame, M., Rua, D., and Greenberg, M. L. (2000). The biosynthesis and functional role of cardiolipin. Prog. Lipid Res. *39*, 257–288.

Schlame, M., Towbin, J. A., Heerdt, P. M., Jehle, R., DiMauro, S., and Blanck, T. J. (2002). Deficiency of tetralinoleoyl-cardiolipin in Barth syndrome. Ann. Neurol. *51*, 634–637.

Sedlak, E., and Robinson, N. C. (1999). Phospholipase A(2) digestion of cardiolipin bound to bovine cytochrome c oxidase alters both activity and quaternary structure. Biochemistry *38*, 14966–14972.

Tanida, I., Hasegawa, A., Iida, H., Ohya, Y., and Anraku, Y. (1995). Cooperation of calcineurin and vacuolar H(+)-ATPase in intracellular Ca2+ homeostasis of yeast cells. J. Biol. Chem. *270*, 10113–10119.

Valianpour, F., Mitsakos, V., Schlemmer, D., Towbin, J. A., Taylor, J. M., Ekert, P. G., Thorburn, D. R., Munnich, A., Wanders, R. J., Barth, P. G., and Vaz, F. M. (2005). Monolysocardiolipins accumulate in Barth syndrome but do not lead to enhanced apoptosis. J. Lipid Res. *46*, 1182–1195.

Varela, J. C., van Beekvelt, C., Planta, R. J., and Mager, W. H. (1992). Osmostress-induced changes in yeast gene expression. Mol. Microbiol. *6*, 2183–2190.

Vaz, F. M., Houtkooper, R. H., Valianpour, F., Barth, P. G., and Wanders, R. J. (2003). Only one splice variant of the human TAZ gene encodes a functional protein with a role in cardiolipin metabolism. J. Biol. Chem. *278*, 43089–43094.

Vida, T. A., and Emr, S. D. (1995). A new vital stain for visualizing vacuolar membrane dynamics and endocytosis in yeast. J. Cell Biol. *128*, 779–792.

Vreken, P., Valianpour, F., Nijtmans, L. G., Grivell, L. A., Plecko, B., Wanders, R. J., and Barth, P. G. (2000). Defective remodeling of cardiolipin and phosphatidylglycerol in Barth syndrome. Biochem. Biophys. Res. Commun. *279*, 378–382.

Weisman, L. S. (2003). Yeast vacuole inheritance and dynamics. Annu. Rev. Genet. *37*, 435–460.

Weisman, L. S., Bacallao, R., and Wickner, W. (1987). Multiple methods of visualizing the yeast vacuole permit evaluation of its morphology and inheritance during the cell cycle. J. Cell Biol. *105*, 1539–1547.

Wickner, W., and Haas, A. (2000). Yeast homotypic vacuole fusion: a window on organelle trafficking mechanisms. Annu. Rev. Biochem. *69*, 247–275.

Yale, J., and Bohnert, H. J. (2001). Transcript expression in *Saccharomyces cerevisiae* at high salinity. J. Biol. Chem. *276*, 15996–16007.

Yamamoto, A., DeWald, D. B., Boronenkov, I. V., Anderson, R. A., Emr, S. D., and Koshland, D. (1995). Novel PI(4)P 5-kinase homologue, Fab1p, essential for normal vacuole function and morphology in yeast. Mol. Biol. Cell *6*, 525–539.

Yoshimoto, H., Saltsman, K., Gasch, A. P., Li, H. X., Ogawa, N., Botstein, D., Brown, P. O., and Cyert, M. S. (2002). Genome-wide analysis of gene expression regulated by the calcineurin/Crz1p signaling pathway in *Saccharomyces cerevisiae*. J. Biol. Chem. *277*, 31079–31088.

Yu, C. A., and Yu, L. (1980). Structural role of phospholipids in ubiquinol-cytochrome c reductase. Biochemistry *19*, 5715–5720.

Zhang, M., Mileykovskaya, E., and Dowhan, W. (2002). Gluing the respiratory chain together. Cardiolipin is required for supercomplex formation in the inner mitochondrial membrane. J. Biol. Chem. *277*, 43553–43556.

Zhang, M., Mileykovskaya, E., and Dowhan, W. (2005). Cardiolipin is essential for organization of complexes III and IV into a supercomplex in intact yeast mitochondria. J. Biol. Chem. *280*, 29403–29408.

Zhong, Q., Gohil, V. M., Ma, L., and Greenberg, M. L. (2004). Absence of cardiolipin results in temperature sensitivity, respiratory defects, and mitochondrial DNA instability independent of pet56. J. Biol. Chem. *279*, 32294–32300.

Zhong, Q., Gvozdenovic-Jeremic, J., Webster, P., Zhou, J., and Greenberg, M. L. (2005). Loss of function of KRE5 suppresses temperature sensitivity of mutants lacking mitochondrial anionic lipids. Mol. Biol. Cell *16*, 665–675.

Zhong, Q., Li, G., Gvozdenovic-Jeremic, J., and Greenberg, M. L. (2007). Up-regulation of the cell integrity pathway in *Saccharomyces cerevisiae* suppresses temperature sensitivity of the pgs1Delta mutant. J. Biol. Chem. *282*, 15946–15953.